

Sizing and Design Tool for Tall Lunar Tower

Kyongchan Song¹, Martin Mikulas², Matthew K. Mahlin¹,
Jacob T. Cassady³

NASA Langley Research Center, Hampton, VA 23681

Tall lunar towers enable direct collection of solar energy using solar panels that can generate power exceeding 50 kW. Tall lunar towers also support solar reflectors and concentrators for solar farms, which enable various mission architectures on the lunar surface. The Tall Lunar Tower project at NASA Langley Research Center is focused on the design, modeling, fabrication, and testing of an assembled tall lunar tower engineering development unit. Presented in this paper is the development of a sizing and design tool for the tall lunar tower. The predicted frequency and buckling responses of the tall lunar tower from the tool are compared with the results obtained from finite element analysis.

I. Nomenclature

AES	=	Advanced Exploration Systems
A_l	=	Cross-section area of longeron
a_1, a_2	=	Principal axes
b	=	Length of longeron
D	=	Lateral deflection of tower
D_i	=	Diameter of tower
D_o	=	Initial lateral imperfection at the top of tower
E_c	=	Elastic modulus of tower material
EDU	=	Engineering Development Unit
FEA	=	Finite Element Analysis
FEM	=	Finite Element Model
FSE	=	Factor of Safety on Euler Buckling of Tower
FSL	=	Factor of Safety on Euler Buckling of Longerons
g	=	Earth gravitational constant
g_f	=	Planetary gravitational factor
GUI	=	Graphical User Interface
iSAT	=	in-Space Assembled Telescope
I_l	=	Longeron moment of inertia
I_x	=	Moment of inertia about the x-axis
I_y	=	Moment of inertia about the y-axis
I_{xy}	=	Product of inertia
I_{a1}	=	Moment of inertia about the principal a1-axis
I_{a2}	=	Moment of inertia about the principal a2-axis
ISRU	=	In-situ resource utilization
JF	=	Factor to account for joint mass
H	=	Height of tower
M_{truss}	=	Mass of tower

¹ Research Aerospace Engineer, Structural Mechanics and Concepts Branch, Mail Stop 190, AIAA Member

² Research Aerospace Engineer, National Institute of Aerospace

³ Research Aerospace Engineer, Flight Software Systems Branch, Mail Stop 064, AIAA Member

M_{PL}	=	Mass of payload at top of tower
L	=	Length of angle flange
\bar{L}	=	Length to thickness ratio of angle flange
P_L	=	Longeron buckling load
P_T	=	Tower Euler buckling load
q	=	Distributed gravitational load of tower
SOA	=	State of the Art
t	=	Thickness of angle flange
TCU	=	Truss Configuration Utility
TLT	=	Tall Lunar Tower
V&V	=	Verification and Validation
β	=	Area reduction factor for battens and diagonals
ρ	=	Density of tower material
θ	=	Tower tilt angle
Δ	=	Tower tip lateral deflection
Δ_0	=	Normalized tip lateral deflection with respect to the initial tip deflection

II. Introduction

The capability to collect energy from solar arrays is limited by the height of the supporting column at lunar polar locations where solar energy cannot be supplied continuously near the surface. In addition, the complex joint systems of typical space-based columns that could support the solar arrays are susceptible to failure in the lunar environment, which includes coarse lunar dust as well as large temperature fluctuations. In order to support the large 50 kW or greater solar arrays needed to collect and provide continuous solar energy [1] at lunar polar locations, NASA Langley Research Center is developing the Tall Lunar Tower (TLT) under the Advanced Exploration Systems (AES) Polaris project.

The TLT project focuses on the design, modeling, fabrication, and testing of an assembled tall lunar tower engineering development unit (EDU). The EDU will include: 1) a truss structure, 2) structural joints, and 3) a robotic assembly system. In the first year of the project, a trade study will be performed focusing on applicable in-Space Assembly (iSA) technologies [2-6] including options for truss structures, structural joints, and robotic tools. With the results of the trade study and rationales in-hand, the team will develop and test prototype robotic tools, co-designed with truss members of a TLT. Sizing of the truss bays and structural members will be determined to allow stowage for flight as well as stability during assembly. In the second year of the project, the effort will focus on refinement and integration of the prototype robotics with the software for autonomous structural assembly to provide a system capable of autonomously assembling a 50-meter-tall tower, in Earth's gravity [7]. The conceptual design of a TLT and assembly concept are shown in Fig. 1. The truss structure will be characterized to ensure that the structure is robust enough to allow traversal of the robotic assembly system, stabilizer deployment, and the expected loading in Earth's gravity. The robotic agent prototype design will be capable of tethered operation around the base of the truss structure, with force feedback and situational awareness. The use of in-situ resource utilization (ISRU) [8] for tower ballast and truss components will be studied for possible future inclusion. Integrated systems testing will conclude with supervised semi-autonomous assembly of the multi-bay truss structure. The second year of the project will conclude with a demonstration of assembling a full-scale 50-meter-tall tower by the TLT system in a laboratory environment.

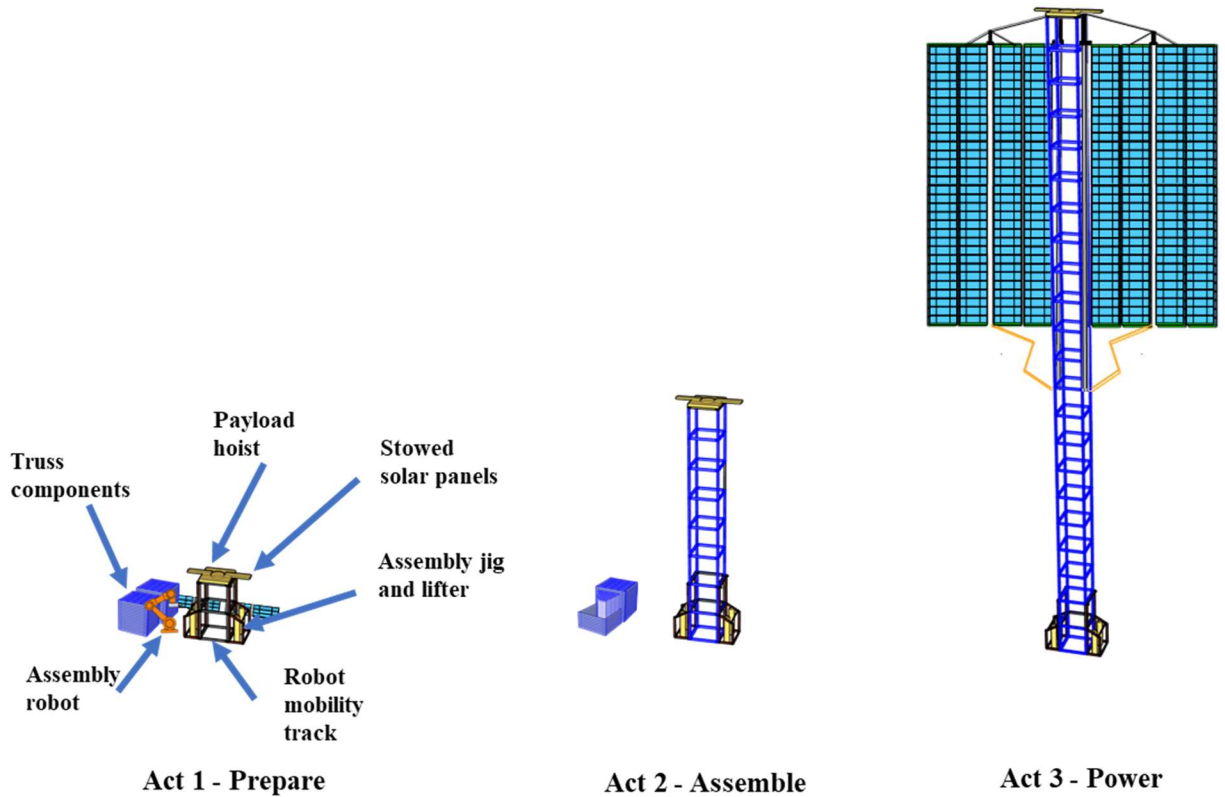


Figure 1. Notional tall lunar tower truss autonomously assembled in the lunar environment.

One of the primary objectives of the TLT project is the development of a TLT sizing tool, called the Truss Configuration Utility (TCU), for assessing the preliminary design and structural requirements on the truss in the lunar environment. The TCU was developed in collaboration with the software and structural design sub-teams. The tool is capable of defining a TLT structure when given a desired tip payload, structure height, and the material properties.

The focus of this paper is on the development of the TCU and verification and validation of the tool versus finite element models (FEMs). Details of the TCU are presented, along with the governing equations. Finally, a selection of predicted responses from the TCU and finite element analysis (FEA) of the TLT, with different modeling parameters, are presented and discussed.

III. Analysis Procedure and Governing Equations of TCU

The TLT design described in this paper is a 50-meter-tall tower, designed to support 50-kW-class solar power generation systems with an equivalent tip mass of 1500 kg. The analysis procedure for the TLT is based on a building block approach established to support the TLT project. The outline of the analysis procedure is shown in Fig. 2.

The TCU was developed to support the preliminary tower design shown in the gray box in Fig. 2. The TCU design tool is capable of defining a lunar tower truss structure when given a desired tip payload, structure height and cross section, and material properties. The TCU provides the truss geometry, including the length, thickness, mass, and volume of the structural members based on the governing equations and input requirements. In the global modeling sizing step, outputs from the TCU are used to build the FEMs and validate the global response of the tower. Once the results from the FEM are used to verify the outputs of the TCU and validates the global response of the tower, the FEM is used for other necessary analyses in the detailed analysis procedure.

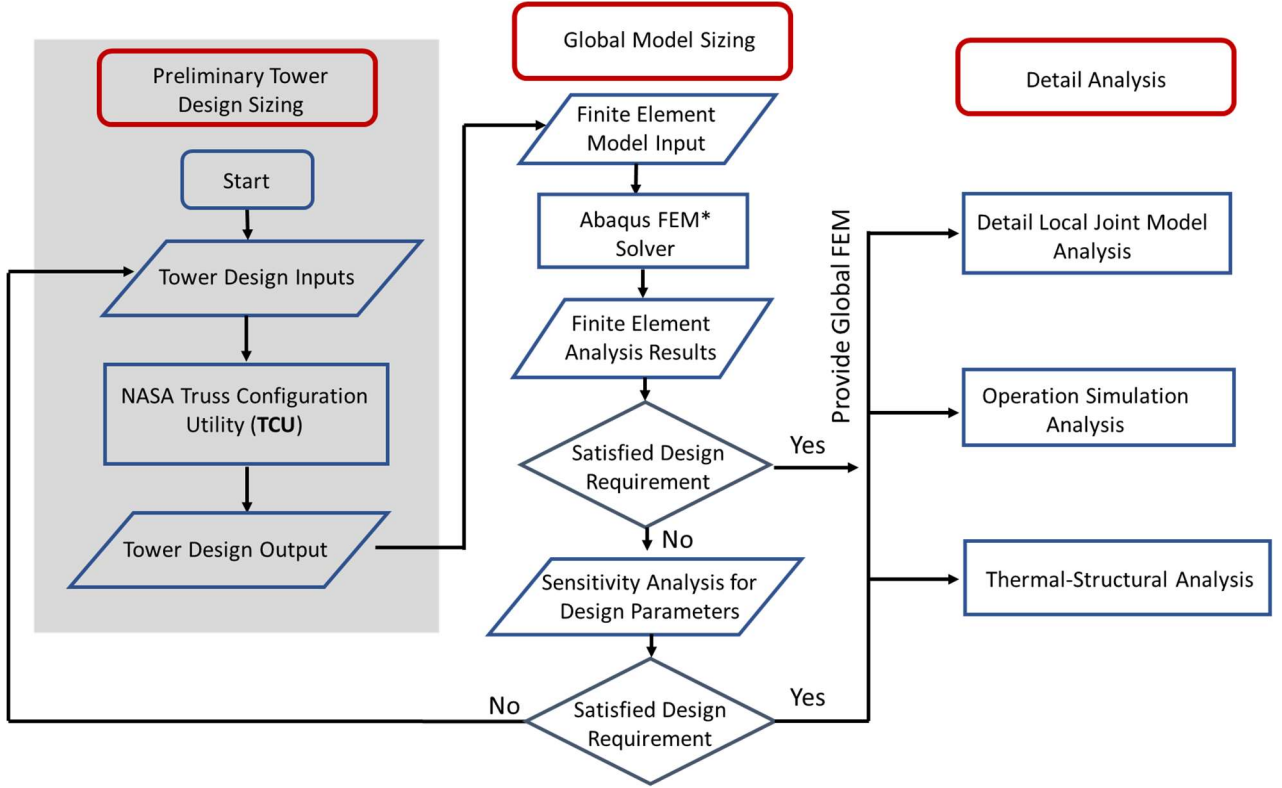


Figure 2. Analysis procedure for a TLT.*

The following assumptions were used for the TCU. First, the TLT is constructed with cubic truss bays. Second, there is no wind loading, and lunar surface gravity is $1/6^{\text{th}}$ of on Earth gravity. Third, the construction site will be leveled and prepared prior to tower construction, with the tower tilt angle set to zero, $\theta = 0$. Fourth, the ratio of height, H , to diameter of the circle which encloses the cross section of tower, D_i , is less than 100, $H/D_i < 100$. In addition, due to a lack of known regolith properties at the site, and possible unexpected disturbances, such as moon quakes, a factor of safety on the Euler buckling of the Tower (FSE) and a factor of safety on the Euler buckling of the Longerons (FSL) are imposed on the governing equations used in the TCU.

The TCU is based on three governing equations: longeron Euler buckling (P_L) and tower Euler buckling (P_T) equations [9], and the mass of the tower (M_{truss}) equation

$$P_L = \frac{\pi^2 E_c I_l}{b^2} = \frac{(M_{PL} + M_{truss}) g g_f}{4} \quad (1)$$

$$P_T = (M_{PL} + 0.3M_{truss}) g g_f = \frac{\pi^2 E_c I_{truss}}{4 H^2} \quad (2)$$

$$M_{truss} = A_l H \rho J F (4 + 4\beta + 5\sqrt{2}\beta) \quad (3)$$

where b = length of the longeron, and $I_{truss} = A_l b^2$, A_l = cross-section area of longeron.

* The use of trademarks or names of manufacturers in this report is for accurate reporting and does not constitute an official endorsement, either expressed or implied, of such products or manufacturers by the National Aeronautics and Space Administration

Three governing equations can be used for a longeron with arbitrary cross-sectional definition. For example, if the cross section of an angle flange longeron is defined as shown in Fig. 3, the moments of inertia and the cross-sectional area of the angle flange longeron can be calculated as

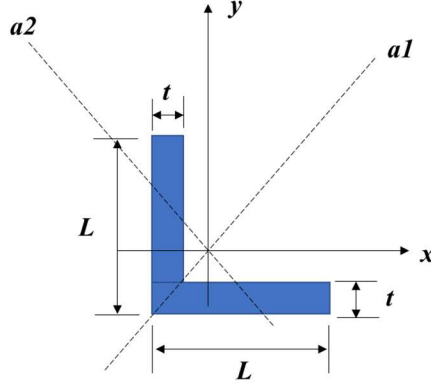


Figure 3. Geometry definition of cross section of an angle flange longeron.

$$I_x = I_y = \frac{t(5L^2 - 5Lt + t^2)(L^2 - Lt + t^2)}{12(2L - t)} \quad (4)$$

$$I_{xy} = \frac{L^2 t(L - t)^2}{4(t - 2L)} \quad (5)$$

$$I_{a1} = \frac{t(2L - t)(2L^2 - 2Lt + t^2)}{12} \quad (6)$$

$$I_{a2} = \frac{t(2L^4 - 4L^3t + 8L^2t^2 - 6Lt^3 + t^4)}{12(2L - t)} \quad (7)$$

$$A_l = 2Lt - t^2 \quad (8)$$

where L and t are the length and thickness of the angle flange, respectively. Using the length-to-thickness ratio ($\bar{L} = L/t$), the area (A_l), and the minimum moment of inertia (I_{a2}) of the cross section can be rewritten as

$$I_{a2} = \frac{t^4(1 - 6\bar{L} + 8\bar{L}^2 - 4\bar{L}^3 + 2\bar{L}^4)}{12(2\bar{L} - 1)} \quad (9)$$

$$A_l = (2\bar{L} - 1)t^2 \quad (10)$$

By substituting Equation 9 into Equation 1 for I_l , and Equation 10 into Equation 2 for A_l , and adding safety factors (FSL and FSE), the governing equations of P_L and P_T for the angle flange longeron can be defined as

$$P_L = \frac{\pi^2 E \frac{t^4(1 - 6\bar{L} + 8\bar{L}^2 - 4\bar{L}^3 + 2\bar{L}^4)}{12(2\bar{L} - 1)}}{b^2 FSL} = \frac{(M_{PL} + M_{truss}) g g_f}{4} \quad (11)$$

$$P_T = (M_{PL} + 0.3M_{truss}) g g_f = \frac{\pi^2 E_c b^2 (2\bar{L} - 1)t^2}{FSE 4 H^2} \quad (12)$$

For the 50-meter TLT, constructed from angle flange aluminum longerons to support 1500 kg top payload, the following input parameters are considered: $E = 70 \times 10^9$ Pa, $\rho = 2700$ kg/m³, $JF = 1.3$, $\beta = 0.7$, $H = 50$ m, $M_{PL} = 1500$ kg, $FSE = 3$, $FSL = 1.5$, $g = 9.8$ m/s², $g_f = 1/6$, $\bar{L} = 10$. Then the two unknown variables of a longeron, b and t , and the mass of the tower, M_{truss} , can be calculated from the three governing equations as $b = 1.088$ m, $t = 2.217$ mm, and $M_{truss} = 192.627$ kg.

For other longeron cross sections, additional input parameters are needed. For example, either the diameter or a thickness of the tube wall is needed for the circular tube longeron. Implementation of the governing equations of TLT in the TCU software is discussed in the following section.

IV. Truss Configuration Utility (TCU) software

The graphical user interface (GUI) for the TCU was developed in Python 3.8 using PySide2 [10] and pyqtgraph [11]. The GUI consists of four main sections: an input section where operators define independent and dependent variables, an output section where solutions to dependent variables are produced and further analysis of the tower is described, a 2-dimensional cross-section display, and a dynamic 3-dimensional representation of the tower. Governing equations were implemented as functions and the nonlinsolve method of the SymPy library [12] was utilized to calculate solutions.

The variables of the input section are dynamic and dependent on the selected tower type. The first column includes check boxes denoting which variables to solve for. Up to three of these variables can be selected at a time. The second column includes the names of the variables. The third column includes the variable symbols from the governing equations. The fourth column allows for user input in the form of drop-down boxes and text edits. Some of the drop-down boxes, such as structure material, are presets that update dependent fields when changed, such as the material density, Poisson’s Ratio, and Young’s Modulus. The fifth column indicates the variable units.

A “Perform Calculations” button at the bottom of the input section initiates the solution procedure filling results into the output section, 2-dimensional cross-section display, and 3-dimensional representation of the tower. In the output section, values solved for using the governing equations are shown in gray while tower analytics such as material volume are shown in white. The 2-dimensional cross-section display and 3-dimensional representation of the tower are generated using the calculated solution. A screenshot of the TCU is provided in Fig. 4, given the description of a 50-meter, aluminum, angle flange tower from the previous section. Note the angle flange struts are displayed as square rods in the 3-dimensional representation of the tower.

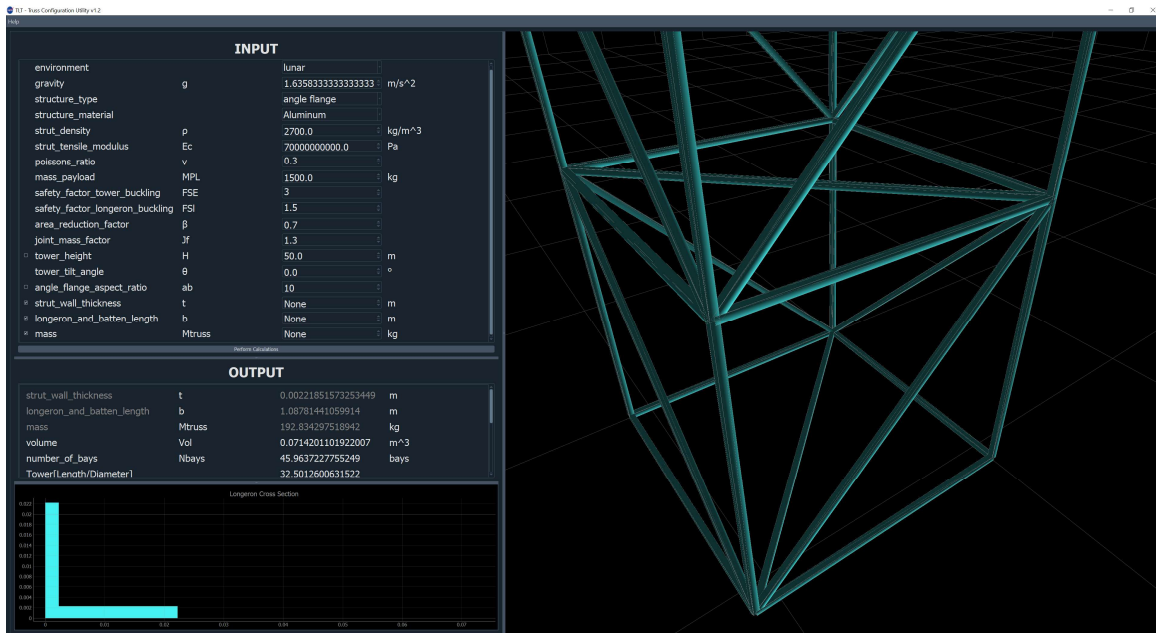


Figure 4. Truss Configuration Utility (TCU).

V. Verification and Validation (V&V) Study of TCU

A verification and validation (V&V) study of the TCU was performed to determine if the TCU accurately sizes the truss structure based on the inputs. In addition, the capability of the TCU to design a lunar tower was demonstrated for a desired tip payload, tower height, longeron cross section, and material selection.

For the V&V study, aluminum TLTs, with a top support payload of 1500 kg were generated from the TCU for four FSEs of 1.1, 1.5, 2, and 3, and five tower heights of 25 m, 50 m, 100 m, 150 m, and 200 m. The cross section of the longeron is the angle flange with $\bar{L}=10$. Other modeling inputs are $JF = 1.3$ and $FSL = 1.5$. Next, FEMs of the

TLTs were developed based on the inputs and outputs of the TCU. In TCU, all displacement components at the bottom four corners are fixed. In the FEMs, all four vertical displacements are constrained as well, but only one corner node is constrained in the remaining two directions. Such as boundary condition constraints TLT at the bottom but prevents lateral overconstraining at the base.

FEA was performed utilizing three different analysis procedures: linear buckling, eigenvalue natural frequency extraction, and static analysis. Estimated mass, buckling loads, natural frequencies and corresponding modes, and mast tip deflection of TLT from FEMs were compared with results from the TCU. The general-purpose finite element software Abaqus/Standard 2021 was used for this work [13].

The estimated mass of the TLTs from both the FEMs and Equation 3 for different FSE and tower heights are presented in Table 1. Estimated TLT masses from Equation 3 are consistent with the estimated FEM masses with less than a 2% difference for all cases.

Table 1. Estimated Mass (kg) of Tower from TCU and FEM.

	25 Meter		50 Meter		100 Meter		150 Meter		200 Meter	
FSE	TCU	FEM	TCU	FEM	TCU	FEM	TCU	FEM	TCU	FEM
1.1	41.7	40.9	135.8	134.5	468.8	467.1	1036.2	1023.7	1941.3	1919.1
1.5	46.3	46.3	151.2	150.6	526.8	524.9	1179.5	1167.7	2246.6	2227.1
2	51.0	51.3	167.2	167.4	587.7	583.1	1333.5	1314.8	2583.6	2554.5
3	58.5	57.8	192.6	191.6	687.3	686.7	1592.9	1586.0	3170.0	3131.2

Predicted tower Euler buckling loads (P_T) were obtained from Equation 12 and compared with P_T from FEA for the different FSE and tower heights considered in this study. Dotted lines in Fig. 5 represent P_T from the TCU, circles represent P_T from FEA, and the blue, orange, green, and black colors represent P_T for four different FSEs of 1.1, 1.5, 2, and 3, respectively. As shown in Fig. 5, P_T increases as the height of tower and FSE increase and predicted P_T of TLT from the TCU and FEA are consistent with less than 4% difference for all cases.

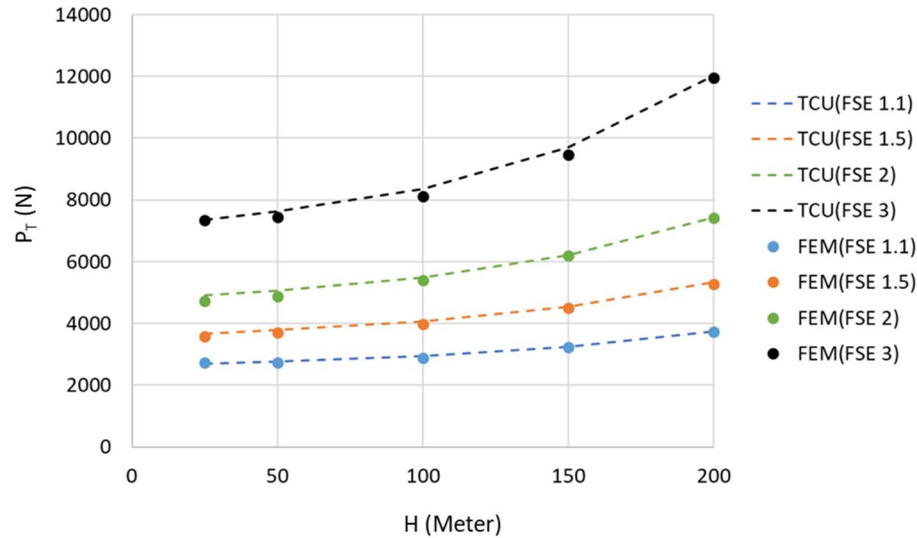


Figure 5. Predicted Euler buckling load, P_T , of tower from TCU and FEA.

A compression load on a column will result in a reduced fundamental frequency and must be considered in the design process of slender columns [14]. In Reference [15], Equation 13 was developed for the fundamental frequency of a vertical cantilevered column subjected to a compressive tip load, M_{PL} , as well as the uniformly distributed gravitational load, q , as shown in Fig. 6.

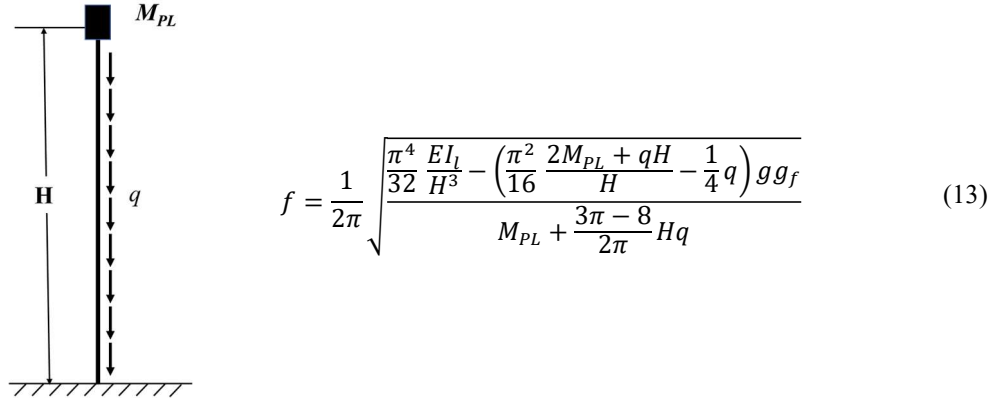


Figure 6. Natural frequency of tower due to tip mass, M_{PL} , and distributed mass, q .

Frequency results from Equation 13 compared to FEA are shown in Fig. 7 for the different FSE and tower heights considered in this study. The predicted fundamental frequency results from Equation 13 and FEA are consistent with less than 10 % difference for a 25-meter-tall tower. The comparison of FEA and Equation 13 results improve as FSE and the height of tower increase. In general, the predicted frequency results from Equation 13 and FEA show consistent results with less than 5 % difference. The impact of FSE on the frequency response of the TLT is presented in Fig. 7 where it can be noted that the frequencies from both Equation 13 and FEA for FSE = 3 are approximately twice as high as the frequencies for FSE = 1.5. This behavior occurs because of the higher EI that results from the higher FSE.

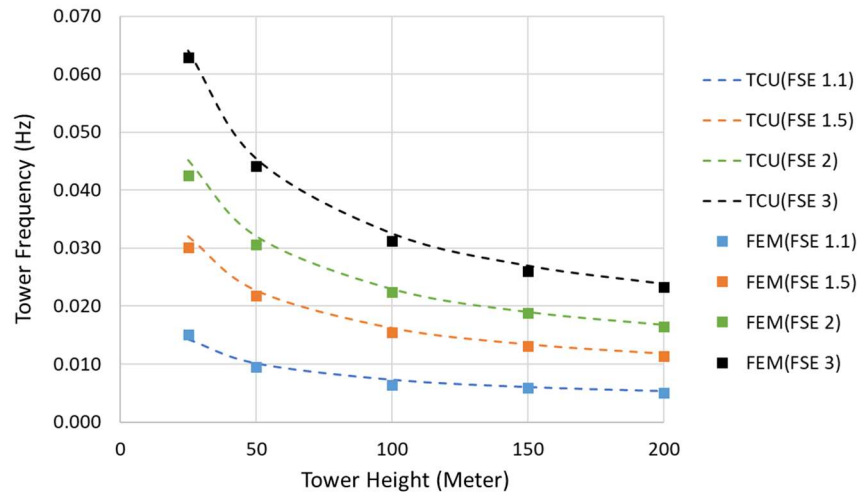
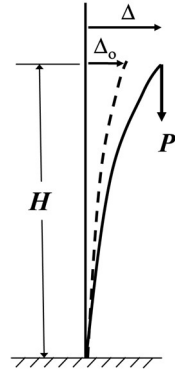


Figure 7. Predicted fundamental frequency of tower due to tip mass, M_{PL} , and distributed mass, q .

The effect of initial stress-free lateral imperfections at the upper tip of the tower, D_o , on the buckling loads was investigated and the relationship between the lateral deflection of the tower tip and FSE was reviewed [14]. The approximate equation that governs the tip deflection magnification from Ref. 9 was used in the V&V study of the TCU, with the Euler factor of safety, FSE, added as prescribed in Equation 14. A diagram of the lateral deflection of the tower is shown in Fig. 8.



$$\frac{\Delta}{\Delta_0} = \frac{1}{1 - \frac{1}{FSE} \frac{P}{P_T}} \quad (14)$$

Figure 8. Lateral deflection of the tower tip.

The FEM of the 25-meter-tall TLT was analyzed to simulate the lateral deflection of the tower. The plot of the tip lateral deflection, Δ , normalized with respect to the initial tip imperfection, Δ_0 , is presented as a function of FSE in Fig. 9. A dotted line in Fig. 9 represents the results from Equation 14 and squares represent the results from FEM.

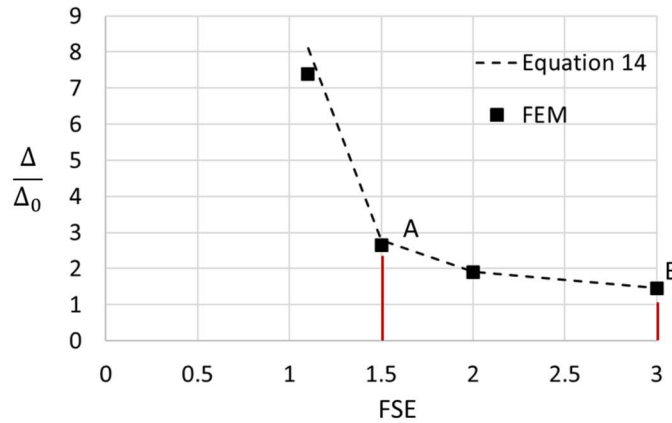


Figure 9. Lateral deflection of the Tower Tip as Function of FSE

Good agreement between the normalized Δ obtained from Equation 14 and using FEA can be observed in Fig. 9; at FSE = 1.5, indicated by point A, the ratio Δ/Δ_0 from Equation 14 is 2.8 and the ratio Δ/Δ_0 from FEA is 2.6; at FSE = 3, indicated by point B, the ratio Δ/Δ_0 from both Equation 14 and FEA is 1.5.

For a V&V study of the TCU, the estimated mass of the TLT from the governing equation was compared with the mass extracted from the FEM and a good agreement was found. Next, three different analysis types were performed and the results from the governing equations and FEA were compared. The comparison of the buckling, fundamental frequency, and static deflection results proved that the implementation of TCU accurately represents governing equations of the truss structure.

VI. Concluding Remarks

The tall lunar tower and the development of a sizing and design tool, the TCU, were presented. Governing equations used in the TCU, and the TCU software, were discussed. FEMs based on the outputs from the TCU were developed for a desired tip payload, structure height, material properties, and FSE. Linear buckling, natural frequency, and static stress FEA were performed to support V&V of the TCU. V&V studies of the TCU using FEA proved that the TCU is capable of defining a TLT structure for a prescribed tip payload, structure height, and material properties.

References

- [1] Mikulas, M., Pappa, R., Warren, J., and Rose, G., “Telescoping Solar Array Concept for Achieving High Packaging,” Proceedings of the 2nd AIAA Spacecraft Structures Conference, Kissimmee, FL, January 2015.
- [2] Dorsey, J. T., Collins, T. J., Doggett, W. R., and Moe, R.V., “Framework for Defining and Assessing Benefits of a Modular Assembly Design Approach for Exploration Systems,” presented at the Space Technology and Applications International Forum – STAIF 2006, Albuquerque, NM, 12-16 February 2006, AIP Conference Proceedings Volume 813, Editor Mohamed S. El-Genk, 2006 American Institute of Physics. <https://doi.org/10.1063/1.2169278>.
- [3] Belvin, W. K., Dorsey, J. T., and Watson, J. J., “Technology Challenges and Opportunities for Very Large In-Space Structural Systems,” presented at the International Symposium on Solar Energy from Space, Toronto, Canada, 8-10 September 2009.
- [4] Dorsey, J. T., Doggett, W. R., Hafley, R. A., Komendera, E., Correll, N., and King, B., “An Efficient and Versatile Means for Assembling and Manufacturing Systems in Space,” presented at the AIAA Space 2012 Conference and Exposition, Pasadena, CA, 11-13 September 2012. <https://doi.org/10.2514/6.2012-5115>.
- [5] Dorsey, J. T., and Watson, J. J., “Space Assembly of Large Structural System Architectures (SALSSA),” presented at the AIAA Space 2016 Conference, Long Beach, CA, 13-16 September 2016. <https://doi.org/10.2514/6.2016-5481>.
- [6] Belvin, W. K., Doggett, W. R., Watson, J. J., Dorsey, J. T., Warren, J. E., Jones, T. C., Komendera, E. E., Mann, T. O., and Bowman, L., “In-Space Structural Assembly: Applications and Technology,” presented at the 2016 AIAA SciTech Forum, San Diego, CA, 4-8 January 2016. <https://doi.org/10.2514/6.2016-2163>
- [7] Mazarico, E., Barker, and Nicholas, J. B., “Advanced Illumination Modeling for Data Analysis and Calibration. Application to the Moon,” *Advances in Space Research*, Volume 62, Issue 11, pp. 3214-3228.
- [8] Clinton, R. G., “Lunar Research for Advanced Manufacturing,” Moon-to-Mars Planetary Autonomous Construction Technology (MMPACT) Physical Sciences Lunar Surface Science Workshop, August 18, 2021.
- [9] Timoshenko, S.P., *Theory of Elastic Stability*, 2nd ed., McGraw-Hill, New York, 1961, pp. 57.
- [10] Qt for Python [Online]. Available: https://wiki.qt.io/Qt_for_Python, Accessed on: Nov. 3, 2022.
- [11] PyQtGraph Scientific Graphics and GUI Library for Python [Online]. Available: <https://www.pyqtgraph.org/>, Accessed on: Nov. 3, 2022.
- [12] SymPy [Online]. Available: <https://www.sympy.org/en/index.html>, Accessed on: Nov. 3, 2022.
- [13] Anon., *ABAQUS™ 2018 Analysis User's Guide, Vols. I-V, Version 2021*, Dassault Systèmes, Providence, RI, 2021.
- [14] Doggett, B. R., Heppler, J., Mahlin, M., Teter, J., Pappa, R., Song, K., White, B., Wong, I., and Mikulas, M., “Towers: Critical Initial Infrastructure for the Moon,” to be presented at the 2023 AIAA SciTech Forum, National Harbor, MD, January 2023.
- [15] Wahrhaftig, A, et al, “The first frequency of cantilevered bars with geometric effect: a mathematical and experimental evaluation”, *J Braz. Soc. Mech. Sci. Eng.*, 2013, 35:457–467.